HHS Public Access

Author manuscript

Clin Cancer Res. Author manuscript; available in PMC 2022 January 29.

Published in final edited form as:

Clin Cancer Res. 2020 March 15; 26(6): 1486–1496. doi:10.1158/1078-0432.CCR-19-2478.

Everolimus inhibits the progression of ductal carcinoma in situ to invasive breast cancer via downregulation of MMP9 expression

Guang Chen[1,2,*], **Xiao-Fei Ding**[1,3], **Kyle Pressley**[1], **Hakim Bouamar**[1], **Bingzhi Wang**[1], **Guixi Zheng**[1], **Larry E. Broome**[1], **Alia Nazarullah**[4], **Andrew Brenner**[5], **Virginia Kaklamani**[5], **Ismail Jatoi**[6], **Lu-Zhe Sun**[1,*]

[1]Departments of Cell Systems & Anatomy, School of Medicine, The University of Texas Health Science Center at San Antonio, San Antonio, TX 78229.

[2]Department of Pharmacology, School of Medicine, Taizhou University, Taizhou, Zhejiang 318000, China.

[3]Laboratory for Biological Medicine, School of Medicine, Taizhou University, Taizhou, Zhejiang 318000, China.

[4]Department of Pathology, School of Medicine, The University of Texas Health Science Center at San Antonio, San Antonio, TX 78229.

[5]Department of Medicine, School of Medicine, The University of Texas Health Science Center at San Antonio, San Antonio, TX 78229.

[6]Department of Surgery, School of Medicine, The University of Texas Health Science Center at San Antonio, San Antonio, TX 78229.

Abstract

Purpose: We evaluated the role of everolimus in the prevention of ductal carcinoma in situ (DCIS) to invasive ductal carcinoma (IDC) progression.

Experimental Design: The effects of everolimus on breast cancer cell invasion, DCIS formation, and DCIS progression to IDC were investigated in a 3D cell culturing model, intraductal DCIS xenograft model, and spontaneous MMTV-Her2/neu mouse model. The effect of everolimus on matrix metalloproteinase 9 (MMP9) expression was determined with Western blotting and immunohistochemistry in these models and in DCIS patients before and after a window trial with rapamycin. Whether MMP9 mediates the inhibition of DCIS progression to

[*]**To whom correspondence and reprint should be addressed:** Guang Chen, Department of Pharmacology, School of Medicine, Taizhou University, 1139 Shi-Fu Avenue, Taizhou, Zhejiang 318000, China, Telephone: +86 15988906927, Fax: +86 576 88665198, gchen@tzc.edu.cn; Lu-Zhe Sun, Department of Cell Systems & Anatomy, School of Medicine University of Texas Health at San Antonio 7703 Floyd Curl Dr., MC7762, San Antonio, TX 78229-3900. Telephone: 210-567-5746, Fax: 210-567-3803. SUNL@uthscsa.edu.

Authors' contributions: G.C., D.X. and L-Z.S. designed research; G.C., D.X., K.P., H.B., B.W., G.Z., and L.B. performed research; A.B., A.N., V.K., I.J., and L-Z.S. participated in the clinical study and patient tissue collection. G.C., D.X. and L-Z.S. analyzed the data; G.C. and L-Z.S. wrote the manuscript.

Disclosure of Potential Conflicts of Interest: The authors have no potential conflicts of interest to disclose.

IDC by everolimus was investigated with knockdown or overexpression of MMP9 in breast cancer cells.

Results: Everolimus significantly inhibited the invasion of human breast cancer cells *in vitro*. Daily intragastric treatment with everolimus for 7 days significantly reduced the number of invasive lesions from intraductal DCIS foci and inhibited DCIS progression to IDC in the MMTV-Her2/neu mouse mammary tumor model. Mechanistically, everolimus treatment decreased the expression of MMP9 in the *in vitro* and *in vivo* models, and in breast tissues from DCIS patients treated with rapamycin for one week. Moreover, overexpression of MMP9 stimulated the invasion whereas knockdown of MMP9 inhibited the invasion of breast cancer cell-formed spheroids *in vitro* and DCIS *in vivo*. Knockdown of MMP9 also nullified the invasion inhibition by everolimus *in vitro* and *in vivo*.

Conclusions: Targeting mTORC1 can inhibit DCIS progression to IDC via MMP9 and may be a potential strategy for DCIS or Early-Stage IDC therapy.

Keywords

DCIS; invasion; mTOR; MIND model; MMP9

Introduction

Breast cancer is the most common cancer in women and is the second cause of cancer-related mortality in the world (www.breastcancer.org). Early detection and timely intervention are main strategies to prevent invasive breast cancer. Ductal carcinoma in situ (DCIS) is the most common type of early-stage breast cancer. DCIS is a nonobligate precursor of invasive breast cancer, and it has been estimated that 14~53% of DCIS cases will progress to invasive breast cancer within 30 years (1). In addition, almost 50% of the DCIS patients who developed invasive breast cancer died of metastatic disease 1–7 years after diagnosis (2,3). DCIS is rarely palpable, and almost all cases are diagnosed with screening mammography (4). Following the implementation of mammography screening in the United States in the early 1980s, the number of DCIS cases increased more than 5-fold in the ensuing 20-year period (5). Consequently, prevention of DCIS progression has become a major topic of interest in the field of breast cancer research and treatment.

Currently, standard therapy for DCIS involves breast conserving surgery with or without radiation and adjuvant hormonal therapy (6), which, however, only reduces the risk of death from invasive breast cancer 10 years later by 0.9% to 0.8%. As such, low efficacy and over-treatment of DCIS are the main concerns with the current practice (7–10). The strategies to address these challenges and to enhance our understanding of DCIS include (3,11–13): (a) identification of which DCIS will develop into invasive breast cancer, (b) optimal treatment for potentially hazardous DCIS, and (c) identification of candidate markers for intervention with optimal treatments.

Mutational activation of PI3K pathway is a major driver of DCIS invasive progression (14). The mammalian target of rapamycin (mTOR) sits in the center of PI3K signal pathway and has been validated as an important anticancer target (15,16). The mTOR

inhibitor everolimus is approved by FDA for the treatment of patients with hormone receptor and HER2 positive breast cancer in combination with exemestane after failure of treatment with letrozole or anastrozole (https://www.pharma.us.novartis.com/product-list/products?title=AFINITOR). Although PI3K pathway activation has been reported in high grade DCIS (17), whether everolimus is efficacious in preventing DCIS to invasive breast cancer remains to be elucidated. Namba *et al* (18). showed that intraperitoneal injection with rapamycin inhibited the growth of premalignant and malignant tumors formed by transplanted preneoplastic and malignant outgrowth in MMTV-PyV-mT transgenic mice providing the preliminary evidence implicating the roles of mTORC1 pathway in DCIS progression.

In this study, we investigated the effect of the rapalog everolimus with improved pharmacokinetics and reduced immunosuppressive effects compared to rapamycin (19) on DCIS progression in 3-D spheroid invasion assays *in vitro* and in two different mouse DCIS models *in vivo*. Our data show that everolimus can abrogate DCIS progression by inhibiting MMP9 expression, which was also observed in breast tissues from DCIS patients enrolled in a neoadjavant trial with rapamycin.

Materials and methods

Cell culture and reagents

MCF-10DCIS.COM cell line was purchased from Wayne State University and maintained in DMEM/F-12 (1:1) culture medium (Gibco) supplemented with 5% horse serum, 1.05 mM $CaCl_2$ and 10 mM HEPES. SUM225 cell line was obtained from Dr. Fariba Behbod (Department of Pathology and Laboratory Medicine. University of Kansas Medical Center) and maintained in DMEM/F-12 (1:1) culture medium (Gibco) supplemented with 5% fetal bovine serum (FBS), 10 mM HEPES (10 mM), hydrocortisone (1 μg/mL) and insulin (5 μg/mL). Cells were cultured in a humidified atmosphere of 95% air plus 5% CO_2 at 37°C. The cell line authentication and Mycoplasma testing were performed annually.

For cell line authentication, DNA from a specific cell line was extracted using QIAamp® DNA Mini Kit (QIAGEN Sciences, Germantown, MD) and used for the profiles of the 10 standard short tandem repeat (STR) markers, D13S317, TH01, D5S818, D16S539, Amelogenin (AMEL), TPOX, D7S820, CSF1PO, vWA, D21S11. The obtained STR profile data of our samples were compared with the standard STR profile through the following website, http://www.sigmaaldrich.com/life-science/cell-culture/cell-culture-products.html?TablePage=15874949, https://www.atcc.org/ and https://www.phe-culturecollections.org.uk/products/index.aspx. Mycoplasma Contamination was detected using MycoAlert™ Mycoplasma Detection Kit (Cat# LT07–118) from Lonza America, Inc. & Arch Chemicals, Inc. (Alpharetta, GA). All cell lines used in this study were mycoplasma-free.

Everolimus was obtained from Selleckchem (Houston, TX). Matrigel™ Basement Membrane Matrix was obtained from BD Biosciences (San Jose, CA).

Expression Vectors

pLenti3 MMP9 and empty vector were obtained from Applied Biological Materials (abm) Inc. (Richmond, BC, CANADA). pLKO.1-MMP9-shRNA (TRCN0000051438) and empty vector were obtained from Sigma (Burlington, MA). The lentivector pLV411G effLuc-flag-IRES-hrGFP containing a luciferase and green fluorescence protein (Luc-GFP) expression cassette was kindly provided by Dr. Brian Rabinovich (UT MD Anderson Cancer Center).

3D assessment of cell invasion

MCF-10DCIS.COM or SUM225 cells (1,000 cells) were gently mixed with 30 μL Matrigel and plated as a droplet containing single cell-Matrigel mixture onto pre-warmed (in a 37°C incubator) 24-well ultra-low attachment plate for invasion assay. After the droplet solidified inside a 37°C incubator for 15 minutes, it was covered with 500 μl complete cell culture medium, and incubated at 37°C for 15 days. Images were acquired and the 3D-spheroids that invaded the matrix and the total number of 3D-spheroids were counted for the calculation of percent invasive organoids.

Mouse Intraductal xenograft model

All animal experiments were conducted following appropriate guidelines. They were approved by the Institutional Animal Care and Use Committee and monitored by the Department of Laboratory Animal Resources at the University of Texas Health Science Center at San Antonio. Intraductal injections of single-cell suspensions were performed as described by Behbod et al (20). Briefly, Luc-GFP expressing SUM225 or SUM225-MMP9 KD cells were suspended in ice cooled PBS at 500 cells/μl with 0.04% trypan blue. A 30-gauge Hamilton syringe, 50-μl capacity, with a blunt-ended 1/2-inch needle was used to deliver the cells. Ten-week-old virgin female nude mice were anesthetized, and a Y-incision was made on the abdomen to allow the skin covering the inguinal mammary fat pads to be peeled back to expose the inguinal glands. The nipple of both inguinal glands was snipped so that the needle can be directly inserted into the mammary duct. Twenty microliters of the cell suspensions were injected. The injection was judged successful when the blue cell solution flew into secondary and tertiary mammary ducts. The skin flap was returned to the original position and closed with wound clips. Ketoprofen cream was applied to the wound and the mouse was laid on a heat pad set for recovery from anesthesia. The wound clips were removed after 7–10 days. The growth of tumor cells in the mammary glands were detected with bioluminescence imaging with a Xenogen IVIS-Spectrum imaging system (Xenogen Corporation) once a week.

The experimental scheme for short-term everolimus treatment is shown in Figure 2J. Briefly, 3 weeks after injection of mammary epithelial cells, mice were ranked based on tumor burden as reflected by total photon flux values from bioluminescence imaging of the injected mammary gland and divided into three groups with matched tumor burden for the treatment with vehicle, low everolimus at 0.5 mg/kg, or high everolimus at 2.5 mg/kg once daily via intragastric gavage for seven days. Everolimus was dissolved in 4% ethanol, 5% PEG400 and 5% Tween 80 at 4 mg/mL. The mammary glands were harvested 10 weeks after intraductal injection and fixed in ethanol.

Whole-mount Carmine staining

Mammary tissues were dissected, spread onto glass slides, and fixed overnight in 100% ethanol at room temperature. Following fixation, the glands were washed with 70% ethanol for 15 min, then rinsed in water and stained overnight in carmine alum staining solution (0.2 % Carmine (Sigma) and 0.5% Aluminum potassium sulphate (Sigma)). Stained glands were soaked sequentially in 70%, 95%, and 100% ethanol each for 15 min. Slides were cleared in 100% xylene for 30 min before mounting.

Immunoblot

After different types of treatment, cells were resuspended in lysis buffer (50 mmol/L Tris-HCl, 150 mmol/L NaCl, 0.5% NP40, 1mmol/L Na_3VO_4, 5 mmol/L NaF, 80 mmol/L B-glycerophosphate). The Thermo Scientific T-PER Tissue Protein Extraction Reagent was used for total protein extraction from mouse mammary gland tissue. About 100 mg tissue was added in a mortar with 10 mL liquid nitrogen, ground into powder. T-PER Reagent (1 mL) was then added and ground with tissue powder. The mixture was transferred to a 1.5 mL Centrifuge tube and centrifuged at 10,000 × g for 5 minutes at 4 °C to pellet cell/tissue debris and collect supernatant protein extracts. Equivalent amounts of proteins (50 μg) were analyzed by SDS-PAGE. Appropriate antibodies to GAPDH (Santa Cruz Biotechnology, Santa Cruz, CA), MMP9 (Invitrogen, Carlsbad, CA), p-P70S6K1 (Cell Signaling Technology, Beverly, MA), and P70S6K1 (Cell Signaling Technology, Beverly, MA) were used. Proteins were visualized with peroxidase-coupled secondary antibody from Sigma-Aldrich (Louis, MO), using Electrochemiluminescence (ECL, ThermoFisher Scientific,Grand Island, NY) solution for detection.

Immunohistochemistry

Tissue sections were rehydrated through xylene and graded concentrations of ethanol (100% ethanol for 5 min for three times, 95% ethanol for 5 min once, 80% ethanol for 5 min once), incubated in sodium citrate (10 mM, pH 6.0) at 95°C for 10 min and then cool down at room temperature, followed with blocking for endogenous peroxidase with 3% hydrogen peroxide (Thermo Fisher Scientific, Waltham, MA, USA) for 30 min in room temperature. Sections were permeabilized with 0.1 % Triton and blocked in 10% goat serum for 30 min. Rabbit anti-MMP9 antibody (Invitrogen, Carlsbad, CA) was diluted at 1:400 in PBS and added to the tissue sections for incubation at 4°C overnight. The tissue sections were then incubated with a biotinylated goat anti-rabbit antibody (1:200, BD Pharmingen, San Diego, CA, USA), followed with color staining using streptavidin-horseradish peroxidase and DAB Substrate Kit (BD Pharmingen, San Diego, CA, USA). The counterstain was done with hematoxylin.

DCIS tissues from patients

We obtained paraffin sections of the biopsy (pre-treatment) and surgical (post-treatment) samples from DCIS patients in The University of Texas Health Science Center at San Antonio, who participated in a clinical study (ClinicalTrials.gov ID: NCT02642094). We obtained written informed consent from every patient who participated in the clinical study. The study was approved by our institutional review board and was carried out in accordance with the Declaration of Helsinki and Good Clinical Practice guidelines.

Statistics

The data were analyzed using the 7th version of Prism (La Jolla, CA). The quantitative data were expressed as mean ± SEM and compared using one-way ANOVA. The tumor incidence data were compared using Chi-square test. $P<0.05$ was considered statistically significant.

Results

Everolimus inhibits invasion of DCIS cells in vitro

Because DCIS progression to invasive breast cancer involves overt invasion of tumor cells across basement membrane surrounding mammary ducts, we investigated the potential of targeting mTOR as a strategy of anti-DCIS invasion. We first tested whether everolimus, one of the classic mTOR inhibitors, could inhibit the invasion of DCIS cells *in vitro*. When MCF-10DCIS.COM or SUM225 cells, which are known to form DCIS inside mouse mammary ducts (20), formed 3D spheroids inside Matrigel, they also formed invasive extensions as shown in Figure 1A. In contrast, treatment with everolimus significantly reduced the number of 3D-spheroids with the invasive extensions (Figure 1A and 1B). More interestingly, while the 100 nM everolimus treatment appeared to inhibit both spheroid growth and invasion, the 10 nM everolimus treatment was apparently more effective in inhibiting spheroid invasion than its growth (Figure 1A and 1B) indicating that the inhibition of invasion by 10 nM everolimus was not dependent on growth inhibition. Consequently, we used the 10 nM everolimus treatment in our subsequent *in vitro* experiments.

Everolimus inhibits growth and progression of DCIS cells in mouse intraductal xenograft model

Because everolimus significantly inhibited the invasive ability of DCIS cell lines *in vitro*, we further examined its inhibitory activity in an intraductal human-in-mouse transplantation model. We injected SUM225 cells into the mammary ducts of female nude mice (Figure 2A, 2D, 2G). SUM225 cells formed DCIS-like structures as early as 3 weeks after injection (Figure 2B, 2E, 2H) and invasive lesions 10 weeks after injection (Figure 2C, 2F, 2I). Therefore, we treated the mice 3 weeks after cell injection with everolimus once daily for 7 days via intragastric gavage, and then harvested the mammary glands 6 weeks later as illustrated in Figure 2J. Currently, the recommended dosage of everolimus (Afinitor) for breast cancer is 10 mg orally once daily. Therefore, we used a clinical equivalent dose of 2.0 mg/kg and a lower dose of 0.5 mg/kg in the animal experiments. The treatment with 2.0 mg/kg everolimus significantly inhibited DCIS progression as measured by the percent of DCIS with invasive cells outside of the mammary duct (Figure 3A). In the vehicle control group, 41.29% ± 8.58% DCIS had invasive foci. Everolimus treatment at 2.0 mg/kg decreased the percentage to 13.22% ± 5.22%, while the percentage for the everolimus treatment group at 0.5 mg/kg was 42.65% ± 6.24%, similar to the control group (Figure 3B), which indicates that everolimus decreased SUM225-MIND invasion in a dose dependent way.

The one-week everolimus treatment also decreased SUM225-MIND growth to some extent as measured by *in vivo* luminescence (Figure 4A), but the difference between the vehicle control and the everolimus treatment groups was not significant due to the large variation

of the data. Interestingly, the response rate as indicated by decreases of photo flux with a one-week everolimus treatment at 2.0 mg/kg/day was about 60% (Figure 4B–4E). In the vehicle control group, the luminescence signal in each mouse kept increasing after injection (Figure D), while in the 2.0 mg/kg everolimus group, the luminescence signal showed time-dependent decrease in 4 of the 7 mice (Figure E). There was a significant difference between the vehicle control and the 2.0 mg/kg everolimus group in the response rate based on Chi-squared test (Figure C).

Everolimus causes tumor regression and inhibits progression of mammary DCIS in MMTV/neu mouse

To confirm the inhibitory effects of everolimus on DCIS progression, we next tested it in the MMTV-Her2/*neu* transgenic mice (FVB/N-Tg(MMTVneu)202Mul/J; The Jackson Laboratory), which express a wild-type HER2/neu allele and develop mammary hyperplasia and tumorigenesis (21). The female mice develop DCIS with a latency of about 13 weeks and most mice form palpable mammary tumors at 17 weeks of age based on our preliminary observation. In the present study, we started a one-week everolimus treatment at 2.0 mg/kg once daily via intragastric gavage in 13-week-old female mice and harvested the mammary glands 4 weeks later (Figure 5A). As shown in Figure 5B and 5C, all control mice had mammary tumors at 17 weeks of age, while the everolimus group only had 50% mammary tumor incidence rate based on whole mount staining (Figure 5C) indicating that short-term everolimus treatment caused tumor regression in this mouse mammary tumor model. In addition, everolimus significantly inhibited DCIS progression. In the vehicle control group, 58.86% ± 18.37% *in situ* lesions had extensive microinvasion, while one-week everolimus treatment decreased the percentage to 25.42% ± 22.18% (Figure 5D and 5E), which indicates that everolimus inhibited MMTV/*neu* DCIS invasion.

mTOR inhibition decreases MMP9 protein levels in DCIS cell line and DCIS tissues from SUM225-MIND, MMTV/neu and DCIS patients.

To reveal the underlying mechanism of blocking DCIS invasion by mTOR inhibition, we investigated the effects of mTOR inhibitor on MMP9, a classic invasion-driver protein (22). As shown in Figure 6A, everolimus treatment not only inhibited the phosphorylation of P70S6K1 (p-P70S6K1), an mTOR substrate, but also decreased MMP9 protein levels in SUM225 cells. Similarly, the one-week everolimus treatment also reduced p-P70S6K1 and MMP9 levels in the mammary tumors from the MMTV/neu mice *in vivo* (Figure 6B). In addition, IHC assays also revealed reduction of MMP9 expression in both SUM225-MIND and MMTV/neu mouse mammary tissues after the treatment with everolimus *in vivo* (Figure 6C and 6D). Finally, we extended our investigation in biopsy (pre-treatment) and surgical (post-treatment) samples from DCIS patients, who participated in a clinical study (ClinicalTrials.gov ID: NCT02642094) and were treated with rapamycin at 2 mg/day for one week before surgery. As shown in Figure 6E, the one-week treatment with rapamycin also reduced MMP9 levels in paired samples from three patients. IHC image quantification data is provided in supplementary Figure 1B to 1D. We quantified MMP-9 staining by measuring the average optical density using ImageJ (d 1.47) software and analyzed all MMP9 IHC data, which showed that everolimus or rapamycin decreased MMP9 protein levels in these models.

MMP9 mediates mTOR-induced DCIS cell invasion

To determine the role of MMP9 in promoting DCIS invasion, we stably transduced an MMP9 cDNA expression lentivector or the empty lentivector into SUM225 cells to study the effects of MMP9 overexpression on DCIS invasion. MMP9 overexpression (Figure 7A) significantly enhanced invasive ability of the SUM225 cells in Matrigel (Figure 7B and 7C). Treatment with everolimus appeared to reduce both endogenous and exogenous MMP9 as shown in Figure 7A and consequently not only reduced the invasion rate of control SUM225 3D-spheroids from 15.85% to 7.61% but also reduced the invasion rate of MMP9-overexpressed SUM225 3D-spheroids from 27.04% to 8.88% (Figure 7B and 7C). Thus, overexpression of MMP9 made SUM225 3D-spheroids more sensitive to everolimus.

Next, we used a specific MMP9 shRNA to knock down MMP9 in SUM225 cell line via lentiviral transduction of a control or a specific MMP9 shRNA vector. As shown in the Figure 8A, MMP9 level was clearly reduced in SUM225 cells transfected with MMP9 shRNA. Knockdown of MMP9 reduced the invasion of SUM225 3D-spheroids through Matrigel, which was not further reduced by everolimus treatment (Figure 8B and 8C). Taken together, these data provide biochemical and biological evidences that everolimus inhibits SUM225 3D-spheroid invasion at least in part through the reduction of MMP9 expression and function.

To validate the above *in vitro* observations *in vivo*, we injected SUM225 control and SUM225 MMP9 knockdown cells into the mammary ducts of female nude mice. Three weeks later, each group was further divided into vehicle control and everolimus treatment groups such that the mean luminescence intensity is matched between the two groups. The mice were treated for one week with vehicle or everolimus at 2.0 mg/kg and their mammary glands were harvested 9 weeks after cell injection. As shown in Figure 8D and 8E, everolimus again significantly reduced the mean invasion rate of SUM225 control MIND from 36.95% to 17.95%. Knockdown of MMP9 resulted in a similar reduction of mean invasion rate of the SUM225 MIND such that everolimus treatment showed no further inhibition of the invasion rate of SUM225-MMP9 knockdown MIND (Figure 8D and 8E). These data are consistent with the *in vitro* data above indicating that everolimus decreased SUM225 invasion largely via the inhibition of MMP9.

Discussion

The activation of the mTOR pathway is involved in breast cancer development and progression (23) and rapalogue everolimus (RAD-001/Afinitor) was approved for the treatment of advanced hormone receptor-positive, HER2-negative breast cancer along with exemestane in postmenopausal women who have already received certain other medicines for their cancer (https://www.us.afinitor.com). mTOR pathway activation could also predict the DCIS invasive progression. The upstream molecule PIK3CA mutations were observed in about 50% of DCIS and act as the mutational driver of invasive breast cancer (14,24). Consequently, phosphorylated AKT and pS6 or 4E-BP1 increased progressively from normal breast epithelium to hyperplasia, abnormal hyperplasia and DCIS to invasive tumor (25,26). Inhibition of the mTOR was also postulated to be a therapeutic strategy for preventing DCIS progression. Here, we showed that everolimus, one of the first

generation of mTORC1 inhibitors, inhibited the invasion of human mammary tumor cell line MCF-10DCIS.COM and SUM225 in a 3-D spheroid invasion assay *in vitro*. This is consistent with the previous report that rapamycin treatment reduced invasion of MCF-7 cells by single cell invasion assay using polycarbonate membrane invasion chambers coated with Matrigel. We further showed that intragastric administration of everolimus inhibited the invasion of SUM225 cell-formed DCIS in mouse intraductal (MIND) xenograft model. Namba *et al* (18) have previously showed that intraperitoneal administration of rapamycin inhibited the growth of transplanted premalignant and malignant mammary lesions *in vivo*, which were derived from MMTV-Py-mT mice. In the current study, we used both spontaneous DCIS to IDC mouse mammary tumor progression model and MIND model of human breast tumor cells by intraductal transplantation, which closely mimics clinical DCIS as DCIS initiates inside the ducts and follow to invasive progression (20,27). Our study was also more focused on tumor invasion rather than growth by treating mice via gavage with everolimus, which is taken orally by patients.

More importantly, our study also revealed a mechanism by which everolimus inhibits the invasive property of DCIS cells. Matrix metalloproteinase (MMP) is a class of enzymes that belong to the zinc-metalloproteinases family involved in the degradation of the extracellular matrix in normal physiological processes, such as embryonic development, angiogenesis, cell migration, as well as in pathological processes, such as arthritis, intracerebral hemorrhage, and metastasis (28). MMP2 and MMP9 are well known MMPs related to both breast cancer metastasis and mTOR signaling (29,30). In this study, we tested whether everolimus decreased those MMPs protein levels and found MMP9, but not MMP2 (supplementary Figure 1A), level was reduced upon everolimus treatment. MMP9 has been found to be associated with breast cancer progression. Rha et al showed sequential production and activation of MMP-9 from early stage breast cancer (DCIS and T1 stage) to T2-T4 stage or with lymphovascular permeation progression tumors (31). Although mTOR pathway is involved in DCIS progression (17,25), the role of MMP9 in mTORC1-mediated DCIS invasive progression has not been reported. Our study showed that everolimus decreased MMP9 expression both in SUM225 cells *in vitro* and SUM225cell-formed DCIS and IDC as well as in MMTV/new mouse mammary glands *in vivo*. More interestingly, a short-term of one-week treatment with rapamycin at 2 mg/day also decreased MMP9 expression in mammary tissues from DCIS patients. These findings are consistent with earlier studies reporting that mTORC1 inhibitors can decrease MMP9 expression (32,33). Our study further showed that SUM225 cells with MMP9 knockdown were less invasive and no longer sensitive to everolimus-induced inhibition of invasion demonstrating that MMP9 plays a major role in DCIS invasion in our models.

Everolimus was approved for cancers treatment and other various conditions including prevention of organ rejection after organ transplant based on its immunosuppressive activity. However, it can cause serious side effects although it is a tumor-targeted agent instead of a cytotoxic drug. For the prevention of early malignant progression such as DCIS progression to IDC, drug safety is a more important issue. Our current study shows that a short-term of seven-day treatment with everolimus appears effective in inhibiting DCIS to IDC and reducing tumor incidence in the mouse models. Currently, DCIS is treated with surgery, radiotherapy, and adjuvant hormonal therapy (for ER positive DCIS). While the approach

is mostly effective, it is invasive. Furthermore, not all cases of DCIS progress to IDC, and many patients who are diagnosed with DCIS are therefore over-treated. For many patients, the potential risks of treatment may therefore outweigh the benefits (34). Thus, there is an urgent need to identify therapeutic regimens that are less invasive and carry fewer side effects than the current standard therapies, yet can prevent DCIS to IBC progression. When compared to the current standard treatments for DCIS, a short course of everolimus alone or in combination with one of the current treatment modalities may ultimately prove to be as efficacious, better tolerated, and have fewer adverse effects on quality of life. Thus, our data supports further clinical testing whether short-term everolimus treatment is efficacious in reducing the incidence of progression from DCIS to IDC.

In conclusion, we have shown that the mTORC1 inhibitor everolimus can inhibit DCIS invasion both *in vitro* and *in vivo* by inhibiting MMP9 expression. This is supported by the fact that MMP9-knockdown cells were more insensitive to everolimus in its inhibition of DCIS invasion. Currently, DCIS is treated with surgery, radiotherapy, and 5-years of endocrine therapy. If short-term everolimus proves to be an effective treatment for DCIS, it may become an attractive alternative to the current standard regimen, which is invasive, prolonged, and carries a very substantial risk of morbidity. We propose that drugs targeting the mTORC1 pathway should be further tested for potential treatment of DCIS or early stage breast cancer.

Supplementary Material

Refer to Web version on PubMed Central for supplementary material.

Acknowledgements:

This work was supported by NIH R01CA192564 grant to L-Z.S. and National Cancer Institute Cancer Center Support Grant P30 CA054174 to the Shared Resources of Optical Imaging and Next Generation Sequencing. The work was also in part funded by Zhejiang provincial public welfare project of China 2018C37109 to G. C. We thank the patients for donating their tissues for our research (ClinicalTrials.gov Identifier: NCT02642094). B.W. was in part supported by a fellowship from Xiangya School of Medicine, Central South University, Hunan, and G.Z. was in part supported by a fellowship from the Qilu Hospital, Shangdong University, Shangdong, China. We thank Dr. Fariba Behbod for providing SUM225 cell line, Dr. Brian Rabinovich for providing Luc-GFP expression vector, and Ms. Marisa Rodriguez and Mr. Michael Garcia for assisting with patient tissue collection.

References

1. Punglia RS, Bifolck K, Golshan M, Lehman C, Collins L, Polyak K, et al. Epidemiology, Biology, Treatment, and Prevention of Ductal Carcinoma In Situ (DCIS). JNCI Cancer Spectr 2018;2:pky063 [PubMed: 30627695]
2. Fu F, Gilmore RC, Jacobs LK. Ductal Carcinoma In Situ. Surg Clin North Am 2018;98:725–45 [PubMed: 30005770]
3. Gorringe KL, Fox SB. Ductal Carcinoma In Situ Biology, Biomarkers, and Diagnosis. Front Oncol 2017;7:248 [PubMed: 29109942]
4. Ernster VL, Wrensch MR, Petrakis NL, King EB, Miike R, Murai J, et al. Benign and malignant breast disease: initial study results of serum and breast fluid analyses of endogenous estrogens. J Natl Cancer Inst 1987;79:949–60 [PubMed: 3479643]
5. Kerlikowske K, Molinaro AM, Gauthier ML, Berman HK, Waldman F, Bennington J, et al. Biomarker expression and risk of subsequent tumors after initial ductal carcinoma in situ diagnosis. J Natl Cancer Inst 2010;102:627–37 [PubMed: 20427430]

6. El Hage Chehade H, Mokbel K. Is Adjuvant Endocrine Therapy Indicated for DCIS Patients After Complete Surgical Excision? Anticancer Res 2018;38:1263–6 [PubMed: 29491049]
7. Feinberg J, Wetstone R, Greenstein D, Borgen P. Is DCIS Overrated? Cancer Treat Res 2018;173:53–72 [PubMed: 29349758]
8. Bijker N, Donker M, Wesseling J, den Heeten GJ, Rutgers EJ. Is DCIS breast cancer, and how do I treat it? Curr Treat Options Oncol 2013;14:75–87 [PubMed: 23239193]
9. Groen EJ, Elshof LE, Visser LL, Rutgers EJT, Winter-Warnars HAO, Lips EH, et al. Finding the balance between over- and under-treatment of ductal carcinoma in situ (DCIS). Breast 2017;31:274–83 [PubMed: 27671693]
10. Nowikiewicz T, Zegarski W, Glowacka-Mrotek I. Overtreatment in surgery - does it concern also the patients with ductal breast carcinoma in situ. Pol Przegl Chir 2018;90:47–51
11. Parikh U, Chhor CM, Mercado CL. Ductal Carcinoma In Situ: The Whole Truth. AJR Am J Roentgenol 2018;210:246–55 [PubMed: 29045181]
12. Matsumoto A, Jinno H, Ando T, Fujii T, Nakamura T, Saito J, et al. Biological markers of invasive breast cancer. Jpn J Clin Oncol 2016;46:99–105 [PubMed: 26486826]
13. Casasent AK, Schalck A, Gao R, Sei E, Long A, Pangburn W, et al. Multiclonal Invasion in Breast Tumors Identified by Topographic Single Cell Sequencing. Cell 2018;172:205–17 e12 [PubMed: 29307488]
14. Pang JB, Savas P, Fellowes AP, Mir Arnau G, Kader T, Vedururu R, et al. Breast ductal carcinoma in situ carry mutational driver events representative of invasive breast cancer. Mod Pathol 2017;30:952–63 [PubMed: 28338653]
15. Bahrami A, Khazaei M, Shahidsales S, Hassanian SM, Hasanzadeh M, Maftouh M, et al. The Therapeutic Potential of PI3K/Akt/mTOR Inhibitors in Breast Cancer: Rational and Progress. Journal of cellular biochemistry 2018;119:213–22 [PubMed: 28513879]
16. Costa RLB, Han HS, Gradishar WJ. Targeting the PI3K/AKT/mTOR pathway in triple-negative breast cancer: a review. Breast cancer research and treatment 2018;169:397–406 [PubMed: 29417298]
17. Sakr RA, Weigelt B, Chandarlapaty S, Andrade VP, Guerini-Rocco E, Giri D, et al. PI3K pathway activation in high-grade ductal carcinoma in situ--implications for progression to invasive breast carcinoma. Clin Cancer Res 2014;20:2326–37 [PubMed: 24634376]
18. Namba R, Young LJ, Abbey CK, Kim L, Damonte P, Borowsky AD, et al. Rapamycin inhibits growth of premalignant and malignant mammary lesions in a mouse model of ductal carcinoma in situ. Clin Cancer Res 2006;12:2613–21 [PubMed: 16638874]
19. Yuan R, Kay A, Berg WJ, Lebwohl D. Targeting tumorigenesis: development and use of mTOR inhibitors in cancer therapy. Journal of hematology & oncology 2009;2:45 [PubMed: 19860903]
20. Behbod F, Kittrell FS, LaMarca H, Edwards D, Kerbawy S, Heestand JC, et al. An intraductal human-in-mouse transplantation model mimics the subtypes of ductal carcinoma in situ. Breast Cancer Res 2009;11:R66 [PubMed: 19735549]
21. Jolicoeur P, Bouchard L, Guimond A, Ste-Marie M, Hanna Z, Dievart A. Use of mouse mammary tumour virus (MMTV)/neu transgenic mice to identify genes collaborating with the c-erbB-2 oncogene in mammary tumour development. Biochemical Society symposium 1998;63:159–65 [PubMed: 9513720]
22. van Kempen LC, Coussens LM. MMP9 potentiates pulmonary metastasis formation. Cancer Cell 2002;2:251–2 [PubMed: 12398887]
23. Hare SH, Harvey AJ. mTOR function and therapeutic targeting in breast cancer. Am J Cancer Res 2017;7:383–404 [PubMed: 28400999]
24. Agahozo MC, Sieuwerts AM, Doebar SC, Verhoef E, Beaufort CM, Ruigrok-Ritstier K, et al. PIK3CA mutations in ductal carcinoma in situ and adjacent invasive breast cancer. Endocr Relat Cancer 2019
25. Zhou X, Tan M, Stone Hawthorne V, Klos KS, Lan KH, Yang Y, et al. Activation of the Akt/mammalian target of rapamycin/4E-BP1 pathway by ErbB2 overexpression predicts tumor progression in breast cancers. Clin Cancer Res 2004;10:6779–88 [PubMed: 15501954]
26. Bose S, Chandran S, Mirocha JM, Bose N. The Akt pathway in human breast cancer: a tissue-array-based analysis. Mod Pathol 2006;19:238–45 [PubMed: 16341149]

27. Doria MT, Maesaka JY, Soares de Azevedo Neto R, de Barros N, Baracat EC, Filassi JR. Development of a Model to Predict Invasiveness in Ductal Carcinoma In Situ Diagnosed by Percutaneous Biopsy-Original Study and Critical Evaluation of the Literature. Clin Breast Cancer 2018

28. Cathcart JM, Cao J. MMP Inhibitors: Past, present and future. Front Biosci (Landmark Ed) 2015;20:1164–78 [PubMed: 25961551]

29. Fan SH, Wang YY, Lu J, Zheng YL, Wu DM, Zhang ZF, et al. CERS2 suppresses tumor cell invasion and is associated with decreased V-ATPase and MMP-2/MMP-9 activities in breast cancer. Journal of cellular biochemistry 2015;116:502–13 [PubMed: 25213553]

30. Cancemi P, Buttacavoli M, Roz E, Feo S. Expression of Alpha-Enolase (ENO1), Myc Promoter-Binding Protein-1 (MBP-1) and Matrix Metalloproteinases (MMP-2 and MMP-9) Reflect the Nature and Aggressiveness of Breast Tumors. Int J Mol Sci 2019;20

31. Rha SY, Kim JH, Roh JK, Lee KS, Min JS, Kim BS, et al. Sequential production and activation of matrix-metalloproteinase-9 (MMP-9) with breast cancer progression. Breast cancer research and treatment 1997;43:175–81 [PubMed: 9131273]

32. Osman B, Akool el S, Doller A, Muller R, Pfeilschifter J, Eberhardt W. Differential modulation of the cytokine-induced MMP-9/TIMP-1 protease-antiprotease system by the mTOR inhibitor rapamycin. Biochem Pharmacol 2011;81:134–43 [PubMed: 20854798]

33. Zeng Y, Yang Y. Piperine depresses the migration progression via downregulating the Akt/mTOR/MMP9 signaling pathway in DU145 cells. Mol Med Rep 2018;17:6363–70 [PubMed: 29488612]

34. Benson JR, Jatoi I, Toi M. Treatment of low-risk ductal carcinoma in situ: is nothing better than something? Lancet Oncol 2016;17:e442–e51 [PubMed: 27733270]

Statement of Translational Relevance

Everolimus was approved for breast cancer treatment. However, whether it is efficacious in preventing ductal carcinoma in situ (DCIS) to invasive ductal carcinoma (IDC) progression remains to be elucidated. Moreover, long-term use of everolimus can cause serious side effects although it is a tumor-targeting agent instead of a cytotoxic drug. For the prevention of early malignant progression such as DCIS progression to IBC, drug safety is of paramount importance, particularly given than DCIS is a nonobligate precursor of IBC. Here, we show a short-term of seven-day treatment with everolimus is effective in inhibiting DCIS progression to IDC and reducing tumor incidence and MMP9 levels in mouse models. The reduction of MMP9 was also observed in breast samples from DCIS patients after a short-term rapamycin treatment (ClinicalTrials.gov ID: NCT02642094). Our data support further clinical testing of whether short-term everolimus treatment is efficacious in blocking the progression from DCIS to IDC.

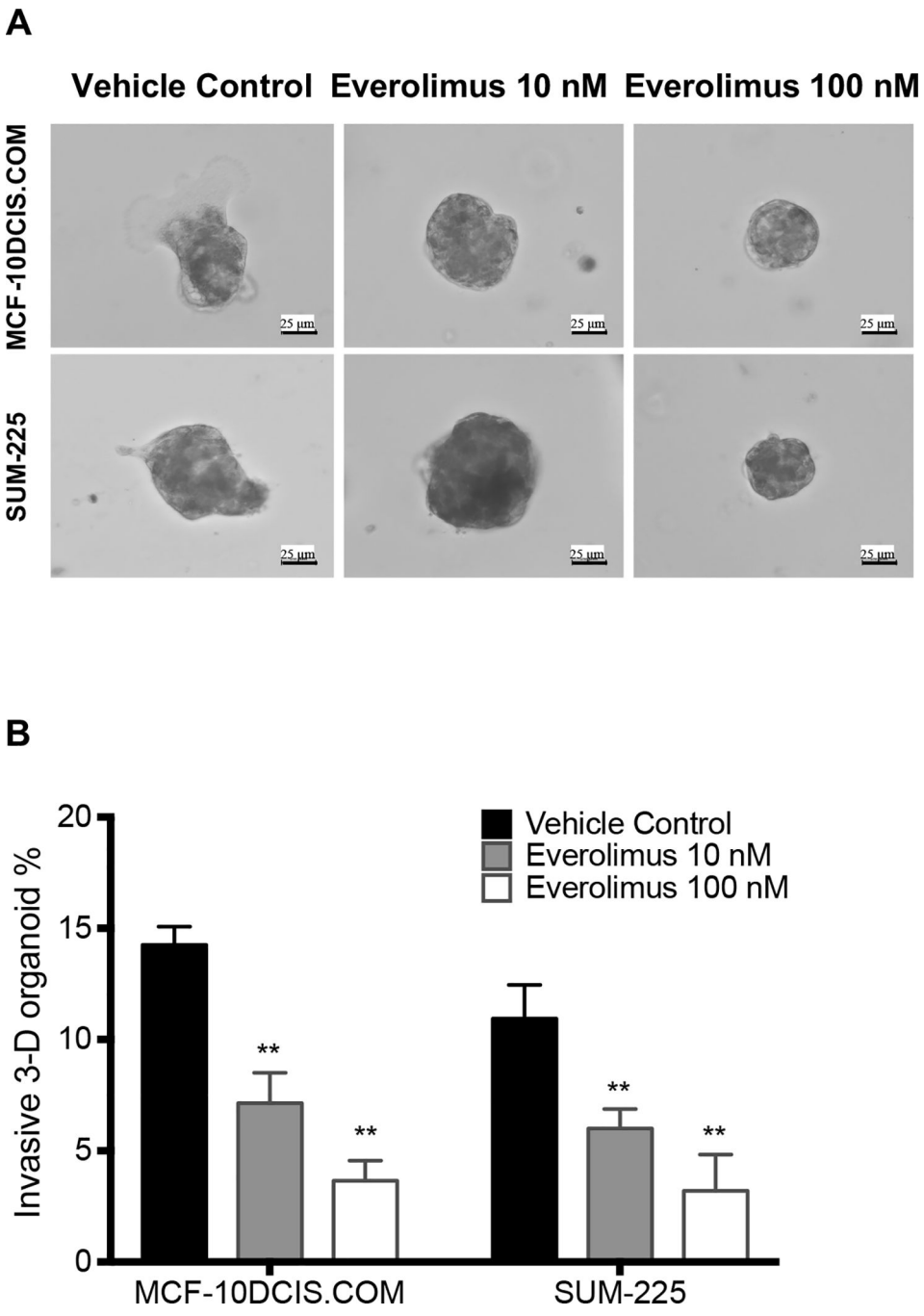

Figure 1.

Everolimus inhibited invasion of 3D-spheroids formed by DCIS cells, MCF-10DCIS.COM or SUM225, through Matrigel. A. Representative Images were acquired with a 20× objective showing invasive extensions from the 3D-spheroids in the control group, but not in the everolimus treatment groups. B. The invasive percentage was calculated by No. of invasive 3D-organoid / No. of total 3D-organoid X 100. Data are shown as means ± SEM, n=3. **p<0.01 vs Vehicle control group with one-way ANOVA.

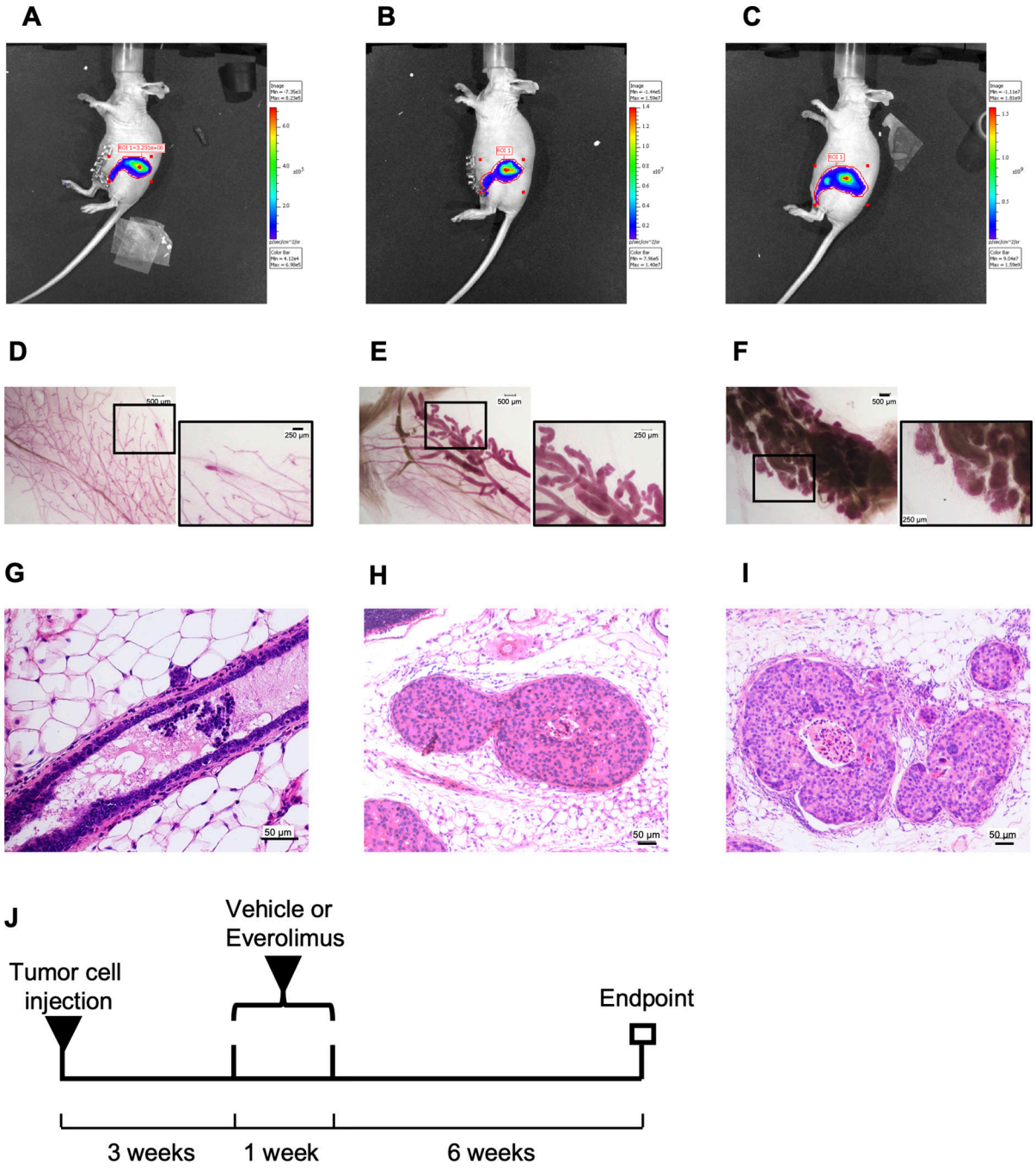

Figure 2.

Experimental scheme for invasive assay in MIND model. (A-C), Tumor growth images of SUM225-MINDs assessed by bioluminescence imaging at one day, 3 weeks and 10 weeks, respectively, after intraductal injection of Luc-GFP expressing SUM225 cells. (D-F), Whole-mount stereo micrographs of representative mammary glands at one day, 3 weeks and 10 weeks, respectively, after intraductal injection of the SUM225 cells. Two images with scale bars of 500 μm or 250 μm for each whole mount are presented. (G-I), H&E staining of representative mammary glands at one day, 3 weeks and 10 weeks, respectively, after

intraductal injection of the SUM225 cells. The scale bar of 25 μm is at the bottom right corner. J, Experimental scheme for short-term everolimus treatment.

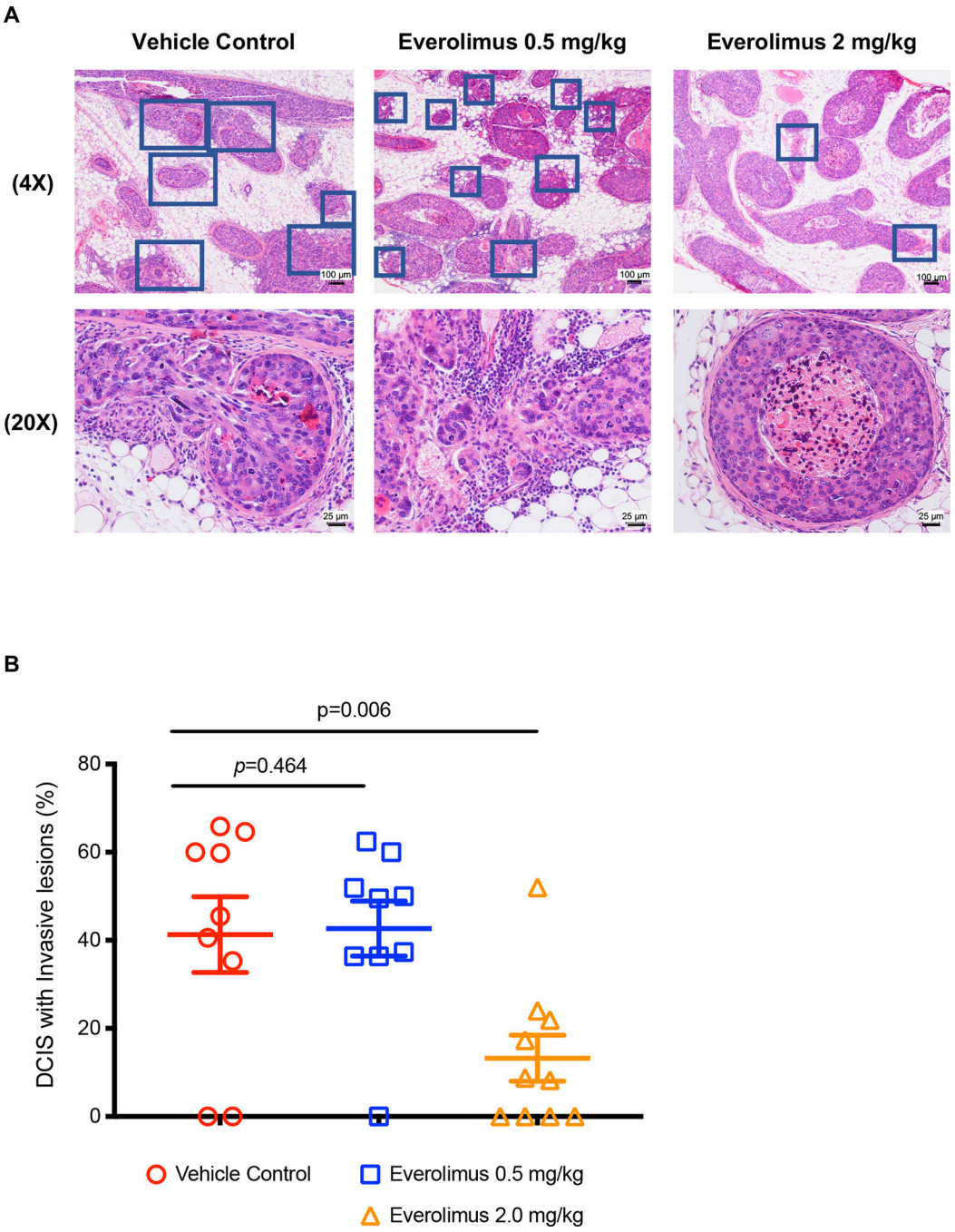

Figure 3.

Everolimus inhibited invasion of SUM225-MIND. A, H&E staining of representative mammary glands 6 weeks after one-week-everolimus treatment. The DCIS lesions with invasive foci are indicated with blue squares. Scale bars: 25 μm or 100 μm. B, The invasive percentage was calculated by No. of DCIS with invasive lesions / No. of total DCIS X 100. Data are shown as means ± SEM. Each data point was obtained from one tissue section from one mouse. P values were obtained from one-way ANOVA between the control and an everolimus group.

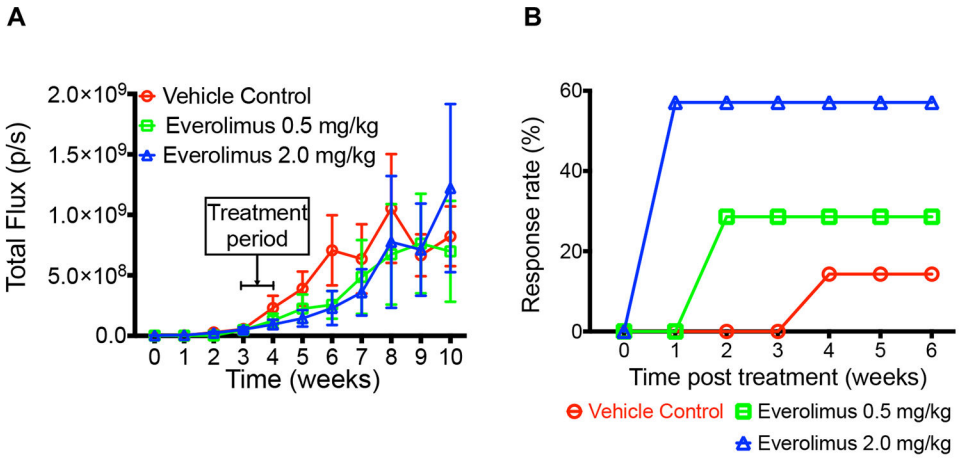

C

		Time (weeks)						
		0	1	2	3	4	5	6
Vehicle	Complete response	0	0	0	0	1	1	1
	No response	7	7	7	7	6	6	6
Everolimus 0.5 mg/kg	Complete response	0	0	0	2	2	2	2
	No response	7	7	7	5	5	5	5
	Chi-square				2.333	2.333	2.333	2.333
	p value				0.127	0.208	0.208	0.208
Everolimus 2.0 mg/kg	Complete response	0	4	4	4	4	4	4
	No response	7	3	3	3	3	3	3
	Chi-square		5.6	5.6	5.6	5.6	5.6	5.6
	p value		0.018	0.018	0.018	0.018	0.018	0.018

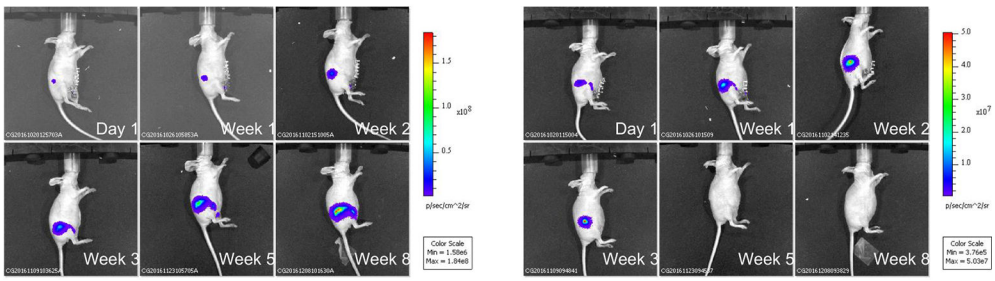

Figure 4.

Everolimus inhibited the growth of SUM225-MIND. A, Tumor growth graph of SUM225-MINDs assessed each week by bioluminescence imaging after intraductal injection of Luc-GFP expressing SUM225 cells. Data are shown as means ± SEM, n=7. B, Percent of mice responded to the one-week everolimus treatment as indicated by bioluminescence signal decrease shown in Panel E. C, Chi-squared test of the response rate. D and E, Representative tumor growth image of SUM225-MINDs assessed by bioluminescence imaging at the

depicted time points after intraductal injection of the SUM225 cells treated with vehicle control (Panel D) or one-week everolimus at 2.0 mg/kg (Panel E) in Week 4.

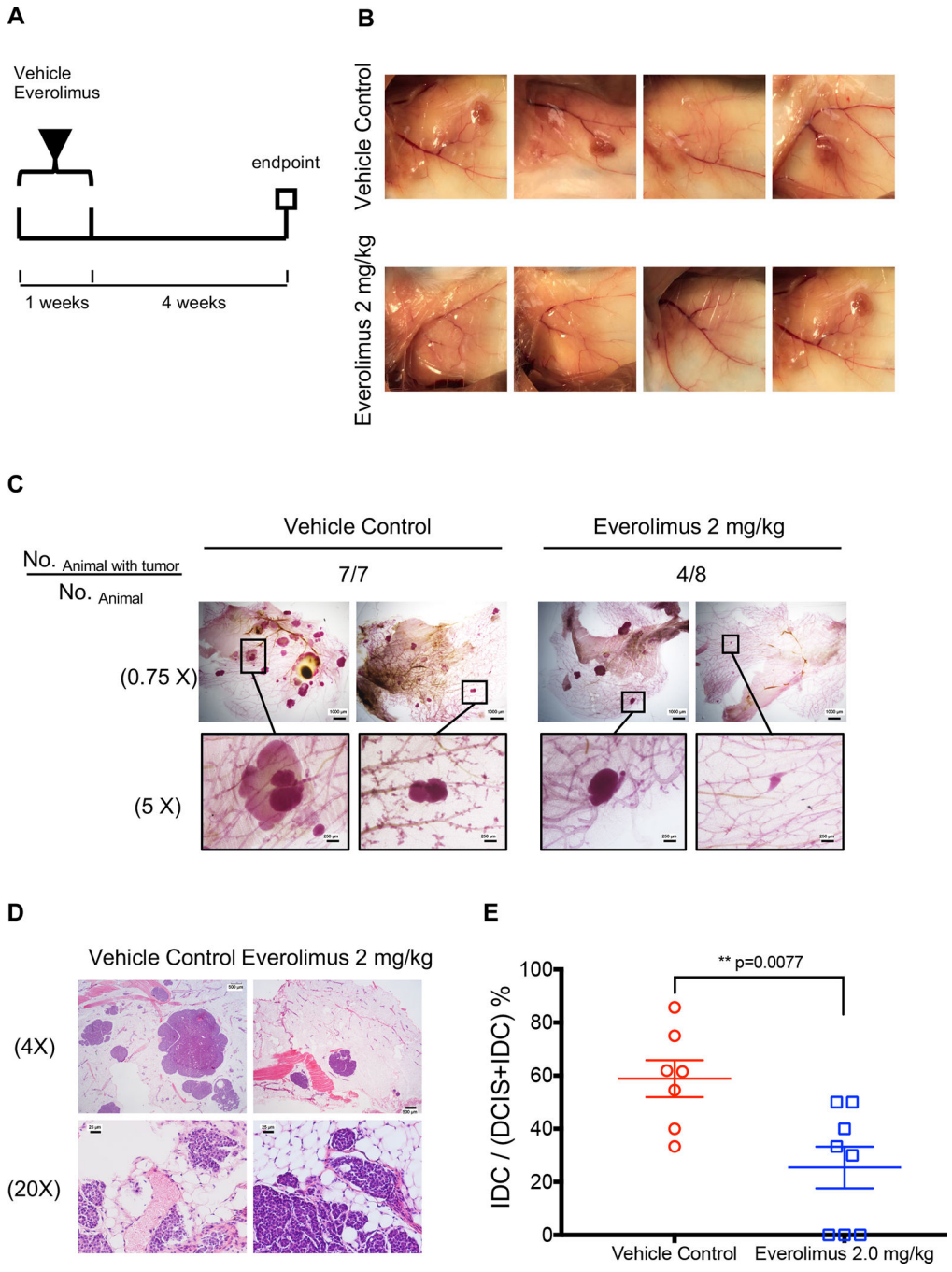

Figure 5.

Everolimus causes tumor regression and inhibits progression of mammary DCIS in MMTV/neu mouse. A, Experimental scheme for short-term everolimus treatment: 13-weeks old female MMTV/neu mice were treated with vehicle control or everolimus for one week. The mice were terminated 4 weeks later. B, Tumor images were captured at the termination of the experiment. C, Whole-mount stereo micrographs of representative mammary glands were acquired with a 0.75X or 5X objective. Scale bars: 250 μm or 1000 μm. D, H&E staining of representative mammary glands at the termination. Scale bars: 25 μm for 20X

magnification or 500 μm for 4X magnification. E, The invasive percentage was calculated by No. IDC / No. of (DCIS and IDC) X 100. Data are shown as means ± SEM. **p<0.01 represents the comparison between control vehicle and everolimus treatment groups, t-test.

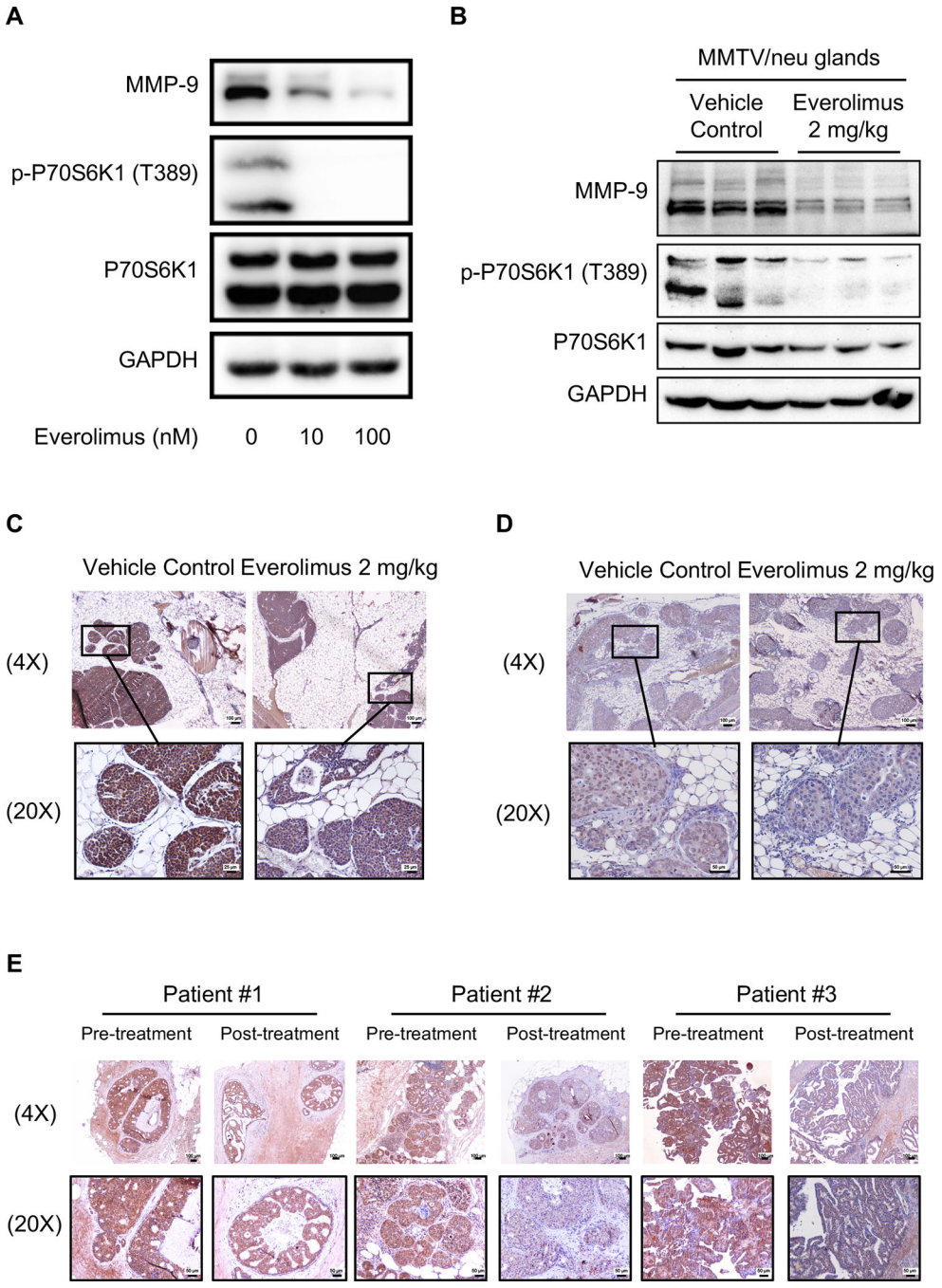

Figure 6.

mTOR inhibition decreases MMP9 expression. A, Everolimus treatment for 24 hours reduced MMP9 protein levels and the phosphorylation of P70S6K1 (p-P70S6K1) in SUM225 cells. B and C, one-week Everolimus treatments at 2 mg/kg/day decreased MMP9 protein levels in the mammary gland of MMTV/neu mice (n=6), detected by WB (B) and IHC (C), Scale bars: 100 μm (4X objective) or 50 μm (20X objective). Each lane represents one mouse mammary tissue in Panel B. D, one-week-Everolimus treatments at 2 mg/kg decreased MMP9 protein levels in the mammary gland of SUM225-MIND mouse mammary

tissues detected by IHC (n=4), Scale bars: 100 μm (4X objective) or 25 μm (20X objective). E, one-week-rapamycin treatments at 2 mg/day reduced MMP9 protein levels in mammary glands of DCIS patients detected by IHC, Scale bars: 100 μm (4X objective) or 50 μm (20X objective).

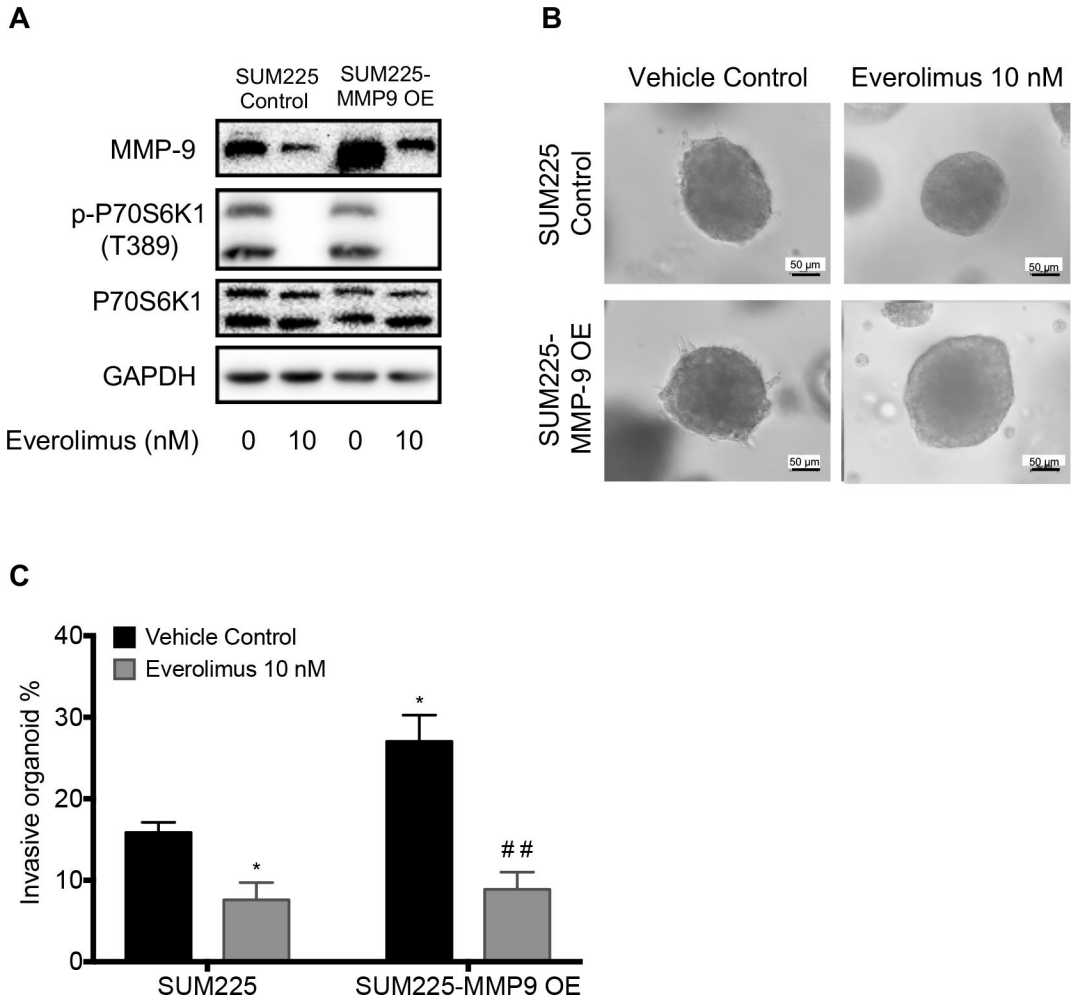

Figure 7.

MMP9 overexpression increased invasion of SUM225 cells and made the cells more sensitive to everolimus inhibition of invasion. A, MMP9 and p-P70S6K1 levels in control vector or MMP9 expression vector transfected SUM225 cells, which were treated wtih 10 nM everolimus for 24 hours. GAPDH is loading control. B, Everolimus inhibited invasion of 3D-spheroids of SUM225 control and MMP9 overexpressing cells through Matrigel. The representative images were acquired with a 20× objective. Scale bars: 50 μm. C, The invasive percentage was calculated by No. of invasive 3D-organoid / No. of total 3D-organoid X 100. Data are presented as means ± SEM, n=3, *$p<0.05$ and ## $p<0.01$ represents the comparison between SUM225 cells transfected with empty vector and everolimus treatment or MMP9 overexpression, or both by one-way ANOVA.

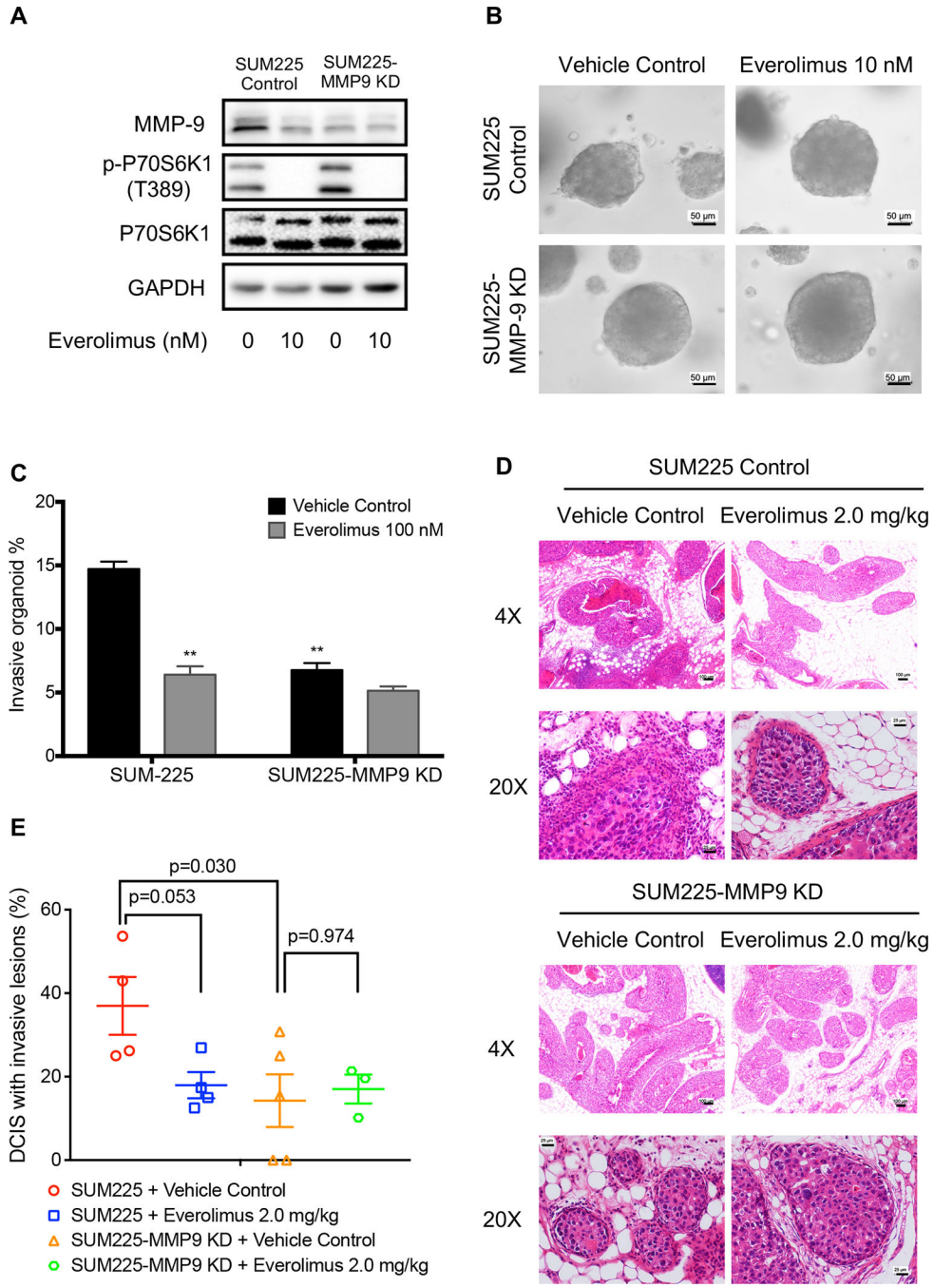

Figure 8.

MMP9 knockdown nullified everolimus activity in blocking the invasion of SUM225 cells both *in vitro* and *in vivo*. A, MMP9 and p-P70S6K1 levels in control or MMP9 shRNA expression vector, which were treated with 10 nM everolimus for 24 hours. GAPDH is loading control. B, Effects of everolimus on invasion of 3D-spheroids of SUM225 control and MMP9 knockdown cells through Matrigel. The representative images were acquired with a 20× objective. Scale bars: 50 μm. C, The invasive percentage was calculated by No. of invasive 3D-organoid / No. of total 3D-organoid X 100. Data are presented as means

± SEM, n=3. *p<0.05 represents the comparison between SUM225 cells transfected with empty vector and everolimus treatment or MMP9 knockdown, respectively, by one-way ANOVA. D, H&E staining of representative mammary glands six weeks after one-week-everolimus treatment. Scale bars: 25 μm (20X magnification) or 100 μm (4X magnification). E, The invasive percentage was calculated by No. of DCIS with invasive lesions / No. of total DCIS X 100, Data are shown as means ± SEM. Each data point represents one mouse. The P values were obtained with one-way ANOVA.